

MATHEMATICAL MODEL OF REED GRIPPER DYNAMICS CONSIDERING FLEXIBILITY OF STEM

Olafs Vronskis, Aivars Kakitis

Latvia University of Life Sciences and Technologies, Latvia
olafs.vronskis@lbtu.lv, aivars.kakitis@lbtu.lv

Abstract. *Phragmites australis* (common reed) is a typical type of wetland vegetation, and is also considered an aggressive vegetation invader in the regional ecosystem. As common reed resources in Latvia are large, they can be used to produce solid biofuels. The stem of the reed is like a natural pipe. It is already used in the production of cocktail straws. However, there is a much wider range of uses, such as toy components etc. Such applications require that the reed stem does not flatten after cutting. Likewise, the end of the stem must be free of sharp edges and smooth. The maximum allowable force for fixing reeds in the gripping mechanism and the stiffness of the reed stem were determined. The parameters obtained were used to determine the dynamic parameters of the gripper. The reed stalk is essentially a flexible cylinder that creates an oscillating transient process during fixation. This reduces the clamping force and can cause failures at the beginning of cutting. This paper presents a dynamic mathematical model for the gripping mechanism, evaluating the flexibility of the reed stem and the friction of the mechanism. The differential equation of motion was obtained using the Lagrange equations. To create a mathematical model, it is necessary to know various parameters of the mechanism. In this study, the geometric parameters of the mechanism, the moments of inertia of the moving parts, the stiffness of the reed and the friction coefficient were determined. These values will be used in the future to simulate the operation of the mechanism in various operating modes.

Keywords: common reed, gripping mechanism, mathematical model, stiffness.

Introduction

Common reed is an undemanding and highly productive aquatic grass widely available worldwide due to its invasive spread [1]. In Europe, reed is one of the most abundant aquatic plants and embodies a major element of the lake flora [2]. Common reed is a native perennial plant growing on wetlands, which is usually used as household feedstock, for thatching roofs and basking mats [3], wall coverings, cocktail straws, Christmas decorations and kids' toys [4]. In order to cut the reeds into the lengths required for cocktail straws, a mechanism is needed to move the reeds to the cutting mechanism.

The aim of this study is to create a differential equation of the dynamics of the clamping mechanism and to determine the necessary parameters for simulation of the mathematical model.

Materials and methods

When it comes to industrial robots, they require special end-effectors called tools. End-effectors can be divided into two major categories, hands and grippers. Hands are multi-finger end-effectors with more than one degree of freedom per finger (Fig. 1 (a) and (b)) and grippers usually have 2 or 3 fingers with one degree of freedom, as shown in Table 1. Hands are designed for general purpose grasps while grippers are designed for more specific tasks [5].



Fig.1. **Hands are multi-finger end-effectors:** a – DLR hand HIT; b – ROBOTIQ Adaptive 3-finger

In most cases, grippers are intended for the implementation of some mechatronic process. Depending on the tasks and work environment, they are designed to perform general operations such as taking, placing or moving products. The tendon-driven gripper [6] has high adaptability but low wear resistance and load capacity, while the worm gear mechanism [7] has high load capacity but low speed and adaptability.

Cylindrical surface gripping mechanisms, in terms of the movement type of the fingers, are divided into two categories (Table 1). Parallel-jaws grippers have the simplest design among grippers, and different designs of them are used in industrial purposes [8]. The 2-finger radial gripper is a compact mechanism designed for use in space-constrained environments. The 3-Finger Angular Gripper is designed for safe gripping of irregular shapes in compact spaces because the fingers pivot inward. The 2-finger parallel gripper is suitable for places where high precision is required, as the linear movement makes it easy to control. The 3-finger centric gripper provides high alignment accuracy for cylindrical, spherical, or uneven parts.

Table 1

Gripping mechanisms

Angular or radial grippers		Parallel or centric grippers	
			
SCHUNK DRG 2-finger radial gripper	SCHUNK SGW 3-finger angular gripper	SCHUNK SPG 2-finger parallel gripper	SCHUNK PZH-plus 3-finger centric gripper

Most usually grippers have two fingers with rotational motions. The system made of a two finger gripper and the work piece is statically indeterminate, if the gripper has three fingers, the system is statically determinate [9].

In previous studies [10], a gripping mechanism was developed to secure the cane in the cutting device (Fig. 2). The study found that the developed reed straw gripping mechanism ensures non-destructive fixing of the straw during reed cutting, if the compressive force generated by the elastic clamps creates sufficient friction force.

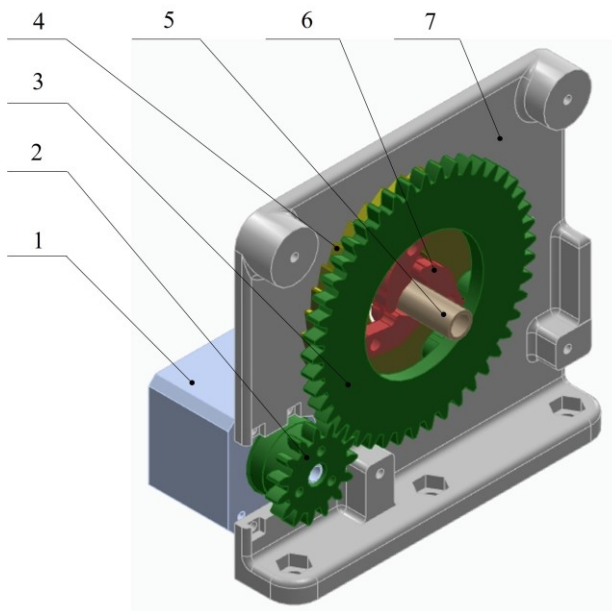


Fig. 2. Common reed gripping mechanism:
 1 – drive mechanism; 2 – drive gear; 3 – driven gear;
 4 – ratchet-wheel; 5 – common reed section;
 6 – lever; 7 – housing

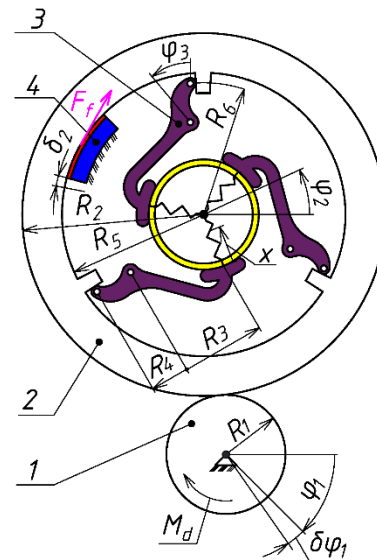


Fig. 3. Kinematic parameters of the gripping mechanism: 1 – drive gear; 2 – driven gear; 3 – lever; 4 – brake

In this study, a differential equation of motion of the gripping mechanism was developed and the necessary quantities for the development of a mathematical model of the mechanism's dynamics were determined. Considering that the reed, which is held in the jaws of the mechanism, is flexible, the clamping mechanism corresponds to a second-order dynamic system. This means that oscillations of the mechanism jaws will occur during the clamping process, which may lead to unstable fixation of the reed stem.

To determine the parameters of the clamping process, a mathematical model of the mechanism was developed. To mathematically describe the mechanism, the Lagrangian function L was used (1) [11]:

$$L = T - U, \quad (1)$$

where T – kinetic energy of the system;
 U – potential energy of the system.

The differential equation of the system is obtained using equation (2):

$$\frac{d}{dt} \left(\frac{\partial L}{\partial \dot{\varphi}_1} \right) - \frac{\partial L}{\partial \varphi_1} = Q_i, \quad (2)$$

where φ_1 – generalized coordinate;
 $\dot{\varphi}_1$ – generalized velocity;
 Q_i – generalized force.

Considering that the drive is powered by an electric motor, the generalized coordinate is chosen as the rotation angle of the driving gear φ_1 (Fig. 3). To determine the Lagrangian function of the system, the system's kinetic and potential energy was calculated. The total kinetic energy of the rotating parts can be determined as the sum of the energies of the individual parts:

$$T = T_1 + T_2 + 3T_3, \quad (3)$$

where T_1 – kinetic energy of the driving gear 1;
 T_2 – kinetic energy of the driven gear 2;
 T_3 – kinetic energy of the lever 3 (Fig. 3).

The elements of the mechanism are in rotational motion; therefore the kinetic energy is determined by equation (4):

$$T_1 = I_1 \frac{\dot{\varphi}_1^2}{2}; T_2 = I_2 \frac{\dot{\varphi}_2^2}{2}; T_3 = I_3 \frac{\dot{\varphi}_3^2}{2}, \quad (4)$$

where I_1, I_2, I_3 – moments of inertia of the rotating bodies;
 $\dot{\varphi}_1; \dot{\varphi}_2; \dot{\varphi}_3$ – angular velocities of the rotating bodies.

The kinetic energies of the individual parts of the mechanism are reduced to the driving gear, which is connected to the motor shaft. By evaluating the kinematic parameters of the mechanism according to the scheme shown in Figure 3, an equation (5) for calculating the total kinetic energy was obtained:

$$T = \left[\frac{I_1}{2} + \frac{I_2}{2} \left(\frac{R_1}{R_2} \right)^2 + 3 \frac{I_3}{2} \left(\frac{R_1}{R_2} \cdot \frac{R_6}{R_3} \right)^2 \right] \dot{\varphi}_1^2, \quad (5)$$

where R_1, R_2, R_3, R_6 , - corresponding radii of rotating parts (Fig. 3).

The potential energy is generated by the elasticity of the reed stem. It is determined by formula (6):

$$U = k \frac{x^2}{2} \quad (6)$$

where x – deformation of the stem during compression;
 k – stiffness coefficient of the reed.

The stem deformation depends on the rotation angle of the presser. Expressing the reed deformation x as a function of the driving gear rotation angle and inserting it into formula 6, the potential energy expression (7) is obtained:

$$U = k \frac{\varphi_1^2}{2} \left(\frac{R_1 R_6 R_4}{R_2 R_3} \right)^2 \tag{7}$$

Substituting into equation (1), the Lagrangian function L is obtained:

$$L = \left[I_1 + I_2 \left(\frac{R_1}{R_2} \right)^2 + I_3 \left(\frac{R_1 R_6}{R_2 R_3} \right)^2 \right] \frac{\dot{\varphi}_1^2}{2} - k \frac{\varphi_1^2}{2} \left(\frac{R_1 R_6 R_4}{R_2 R_3} \right)^2 \tag{8}$$

The generalized force Q_i is determined by assigning a virtual displacement δ_i and calculating virtual work. Considering that the virtual work is done by the torque of the motor and the force of viscous friction, the generalized force is calculated by formula (9):

$$Q_i = M_d - c \dot{\varphi}_1 R_5^2 \left(\frac{R_1}{R_2} \right)^2 \tag{9}$$

where c – coefficient of viscous friction;
 M_d – driving torque of the motor.

Inserting the obtained quantities L and Q_i into equation (2) and performing differentiation, the differential equation of the mechanism 10 was obtained:

$$\left(I_1 + I_2 \left(\frac{R_1}{R_2} \right)^2 + 3I_3 \left(\frac{R_1 R_6}{R_2 R_3} \right)^2 \right) \cdot \ddot{\varphi}_1 = M_d - k \varphi_1 \left(\frac{R_1 R_6 R_4}{R_2 R_3} \right)^2 - c \dot{\varphi}_1 R_5^2 \left(\frac{R_1}{R_2} \right)^2. \tag{10}$$

Assuming that the basic differential equation of rotation is $I_{red} \ddot{\varphi}_1 = \sum_{i=1}^n M_i$, we can determine the reduced moment of inertia I_{red} of the mechanism and the moment of active forces acting on the shaft of the driving motor:

$$I_{red} = I_1 + I_2 \left(\frac{R_1}{R_2} \right)^2 + 3I_3 \left(\frac{R_1 R_6}{R_2 R_3} \right)^2; \tag{11}$$

$$\sum_{i=1}^n M_i = M_d - k \varphi_1 \left(\frac{R_1 R_6 R_4}{R_2 R_3} \right)^2 - c \dot{\varphi}_1 R_5^2 \left(\frac{R_1}{R_2} \right)^2 \tag{12}$$

These quantities are essential for the formulation of a mathematical model describing the mechanism dynamics, with consideration of the electric motor parameters.

To create a mathematical model, it is necessary to determine the geometric parameters of the gripping mechanism and the elasticity coefficient of the reed stem, the moment of inertia, as well as the displacement of the pawl depending on the angle of rotation of the pinion.

In determining the elasticity coefficient, the authors assumed that the reed behaves like a spring during the compression process. Hooke’s law was used to determine the elasticity coefficient of the spring. In previous studies [10], the compressive strength of reed rods in the transverse direction was determined depending on the diameter of the stem.



Fig. 4. Common reed section before loading and points of application of force F and reactions R [10]

The specimens were placed between the fixtures, one of which was flat and the other formed with a cut-out at an angle of 60 degrees, Fig. 4. In this way, the distribution of forces in the jaws of the developed mechanism was simulated. The elastic deformation region was estimated from the force-deformation diagrams obtained in the experiment. The elastic coefficient of the reed was calculated from the obtained results.

The mechanism design was created using the *Solid Edge* computer program. The moments of inertia of the moving parts were determined using *Solid Edge* tools.

Results and discussion

The stiffness of the reed was determined from the linear region of the force-deformation curves [10] using equation:

$$k = \frac{|\Delta F|}{|\Delta h|} = \frac{F}{h_2 - h_1}, \quad (13)$$

where F – pressing force at the end of linear region;
 h_2 – position of testing machine grips at the end of pressing;
 h_1 – position of testing machine grips at the beginning of pressing. Initial force is assumed $F_0 = 0$.

Transverse strength of reed stalks was assessed with using an Instron 5969 universal testing machine. The measurement error of displacement is $\pm 0.1\%$. Average force measuring accuracy did not exceed $\pm 0.5\%$. The reed stem outer diameters were measured using a digital calliper with resolution 0.01mm. The variation of the diameters of each group of the samples did not exceed $\pm 0.2\text{mm}$ [10].

The results obtained are summarized in Table 2. Evaluation of the data indicates that the stiffness increases with increasing the reed diameter. This behaviour can be attributed to the fact that, as the reed diameter increases, the stem wall thickness also tends to increase proportionally, leading to increased resistance to deformation in the radial direction and, consequently, a higher stiffness.

Table 2

Stiffness of reed stems ($\text{kN}\cdot\text{mm}^{-1}$)

Diameter of reed, mm	6 ± 0.2	7 ± 0.2	8 ± 0.2	9 ± 0.2	10 ± 0.2
Position before compression h_1 , mm	6.1 ± 0.1	4.0 ± 0.1	4.5 ± 0.1	3.5 ± 0.1	3.6 ± 0.1
Position after compression h_2 , mm	5.6 ± 0.1	3.5 ± 0.1	4.0 ± 0.1	3.0 ± 0.1	3.1 ± 0.1
Loading force, N	23.1 ± 1.2	24.0 ± 1.3	28.0 ± 1.2	36.0 ± 1.2	35.1 ± 1.3
Stiffness, $\text{N}\cdot\text{mm}^{-1}$	46.2 ± 2.3	48.0 ± 2.5	57.1 ± 2.8	72.6 ± 3.5	70.0 ± 3.4

Microsoft Excel is used to carry out the statistical analysis of the results. Analysis of variance (ANOVA) was used to analyse the differences between the groups. The results of the statistical analysis of the data are summarized in Table 2. The null hypothesis that the average applied force did not depend on the reed diameter was rejected and the alternative hypothesis that the average applied force depends on the reed diameter was accepted.

Table 3

Analysis of variance (ANOVA)

Source of variation	SS	df	MS	$F_{fact.}$	P-value	$F_{crit.}$
Between groups	6482.116	1	6482.116	88.65523	0.000	5.317655
Within groups	584.928	8	73.116	–	–	–
Total	7067.044	9	–	–	–	–

After performing the analysis, it can be concluded that $F_{fact.} = 88.65523 > F_{crit.} = 5.317655$, then with a probability of 95% the null hypothesis can be rejected. The alternative hypothesis that the stiffness of reed stems depends on the reed diameter can be accepted.

The graph in Figure 5 indicates that the reed stiffness depends linearly on the reed diameter. The coefficient of determination is $R^2 = 0.88$. This is large enough to use this relationship in a mathematical model simulation.

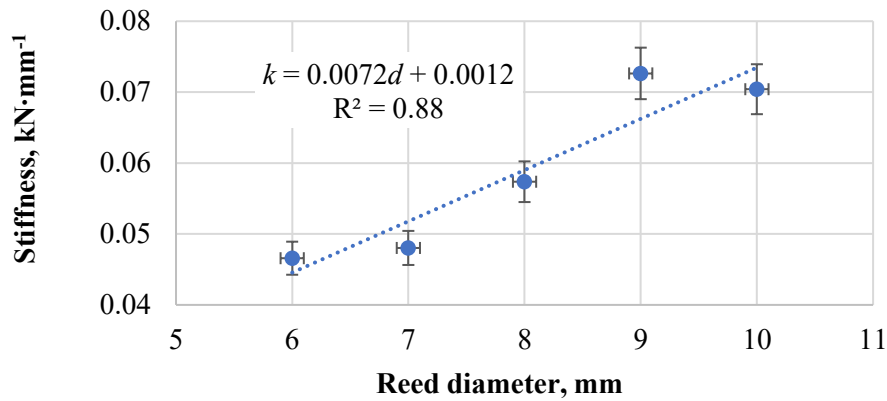


Fig. 5. Relationship between the stiffness and the diameter of reed stems

The design of the gripping mechanism was created in Solid Edge. The model of the gripper is intended to be made using 3D printing of ABS material. The physical properties of the gripper parts were determined using data from the Solid Edge model (Table 4).

Table 4

Physical properties of gripper mechanism parts

Density, g·cm⁻³	1.024	1.024	1.024	1.024
Mass, g	29.2	24.4	1.9	5.2
Mass moment of inertia, g·cm⁻²	306.1	313.2	2.4	5.7
Volume, cm³	28.56	23.83	1.82	5.11
Surface area, cm²	142.39	131.63	12.83	32.93
Elements of the gripping mechanism	 ratchet-wheel	 driven gear	 pawl	 drive gear

To develop a mathematical model, it is necessary to establish the relationship between the rotation angle of the driven gear and the displacement of the oppressor, which represents the reed deformation x (Fig. 3). This can be done in several ways.

The geometric transformation of the gripper can be described either analytically, using the kinematic equations of the mechanism, or empirically, by establishing a relationship between reed deformation and the gear rotation angle based on a Solid Edge model. In this study, the dependence of reed deformation on the gear rotation angle was determined through parametric modelling conducted in the Solid Edge software environment (Fig.7).

The derived regression equation is applicable for the development of the mathematical model. The coefficient of determination, $R^2 = 0.9956$, indicates a high level of correlation, ensuring the model's validity in representing the actual system behaviour. Future research will extend this work by developing a comprehensive dynamic model of the gripper mechanism, incorporating its interaction with the drive motor to capture the full system behaviour.

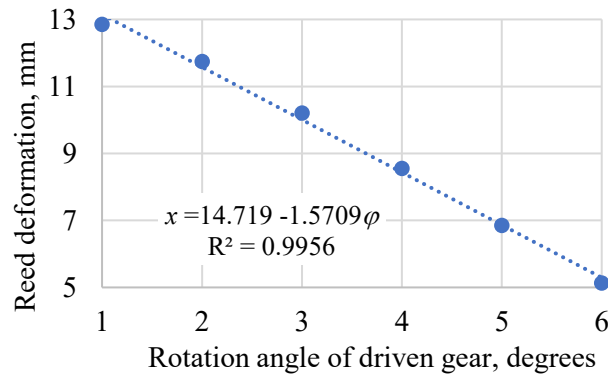


Fig. 7. Deformation of the reed stem depending on the angle of rotation of the driven gear

Conclusions

1. By applying the Lagrangian method, the equations of motion were derived for use in the dynamic model of the reed gripper, enabling the analysis of the mechanism's motion while considering elastic components, frictional forces, and the inertia of the system.
2. The study identified the necessary parameters for developing a mathematical model: the elasticity coefficient of the reed, the moments of inertia, and the deformation of the reed depending on the angle of rotation of the gear.
3. The coefficient of elasticity of reed depends on the diameter of the stem and varies from 0.047 to 0.070 kN·mm⁻¹.
4. The reed deformation changes by 7 millimetres when the gear rotation angle changes by 6 degrees. This is enough to be able to fix reeds with a diameter of 6 to 10 mm in the gripper.
5. The obtained equations and parameters allow to develop a gripper dynamics model, perform simulations, and determine the dynamic parameters of the mechanism.

Author contributions

Conceptualization and methodology, A.K.; validation, A.K.; investigation and data curation, O.V.; writing - original draft preparation, O.V.; writing - review and editing, A.K. and O.V. All authors have read and agreed to the published version of the manuscript.

References

- [1] El-Ramady H.R., Abdalla N., Alshaal T., Fári M., Prokisch J., Pilon-Smits E.A.H, Domokos-Szabolcsy É. Selenium phytoremediation by Giant Reed. In: Lichtfouse E, Schwarzbauer J, Robert D (eds) Hydrogen production and remediation of carbon and pollutants. Springer, Cham, 2015, pp. 133-198.
- [2] Srivastava J., Kalra S.J.S., Naraian R. Environmental perspectives of Phragmites australis (Cav.) Trin. Ex Steudel. Appl Water Sci 4: 2014, pp. 193-202.
- [3] Shuai W., Chen N., Li B., Zhou D., Gao J. Life cycle assessment of common reed (Phragmites australis (Cav) Trin. ex Steud) cellulosic bioethanol in Jiangsu Province, China. Biomass Bioenergy 92: 2016, pp. 40-47.
- [4] Nulle I., Kakitis A., Vronskis O., Smits M. Cutting the common reed stalk while maintaining its cross-sectional shape. Proceedings of International conference "Engineering for rural development", May 20-22, 2020, Jelgava, Latvia, pp. 357-361.
- [5] Honarpardaz M., Tarkian M., Olvander J., Feng X. Finger Design Automation for Industrial Robot Grippers: A review, Robotics and autonomous systems, 87, 2017, pp. 104-119.
- [6] Ciocarlie M., Hicks F. M., Stanford S., Kinetic and Dimensional Optimization for a Tendon-driven Gripper. International Conference on Robotics and Automation, 2013., pp. 2736 -2743.
- [7] Kakogawa A., et al., Underactuated modular finger with pull-in mechanism for a robotic gripper. ROBIO, 2016., pp. 556-561.
- [8] Wolf A., Steinmann R., Schnk H. Grippers in motion. Springer Science & Business Media, 2006, pp. 242.

- [9] Simionescu I., Ion I. Mathematical Models of Grippers. Proceedings of the 10th WSEAS International Conference on “Mathematical and computational methods in science and engineering”, November 7-9, 2008, Bucharest, Romania, pp. 400-403.
- [10] Vronskis O., Kakitis A., Nulle I., Smits M. Evaluation of the transverse strength of reed stalks. International scientific conference “Engineering for rural development”: proceedings, Jelgava, Latvia, May 25-27, Vol.21, 2022, pp. 612-617.
- [11] Goldstein, H., Poole, C., Safko, J. Classical Mechanics (3rd ed.). Boston: Addison-Wesley. 2002. ISBN: 978-0201657029